

Transmit Beampattern Synthesis for MIMO Radar with One-Bit DACs

Tong Wei, Bin Liao, Peng Xiao
College of Electronics and Information Engineering
Shenzhen University
Shenzhen 518060, China
e-mail: binliao@szu.edu.cn

Ziyang Cheng
School of Information and Communication Engineering
University of Electronic Science and Technology of China
Chengdu 611731, China
e-mail: zeeyoungcheng@163.com

Abstract—In this paper, the problem of transmit beampattern synthesis (i.e., transmit beamforming) in multiple input multiple output (MIMO) radar which deploys one-bit digital-to-analog converters (DACs) is investigated. We aim to design appropriate transmit signal sequences, which are quantized by one-bit DACs, such that the amount of transmit energy can be focused into mainlobe region as much as possible, meanwhile, the leakage power of sidelobe region is minimized. It is shown that these requirements can be simultaneously fulfilled by minimizing the integrated sidelobe to mainlobe ratio (ISMR) of transmit beampattern with discrete binary constraints. According to this concept, we utilize the alternating direction multiplier method (ADMM) framework to solve the resulting nonconvex problem. Simulation results will demonstrate the effectiveness and improved performance of the proposed method.

Index Terms—Multiple-input multiple-output (MIMO) radar, transmit beampattern synthesis, one-bit DAC.

I. INTRODUCTION

Inspired by unique advantages of multiple-input multiple-output (MIMO) communication techniques [1], MIMO radar deploys multiple transmit antennas to radiate different waveform sequences, which is also considered as the main difference with phased array radar. Meanwhile, the multiple receive antennas can simultaneously capture those signals reflected back from the target(s). Consequently, by sufficiently utilizing the superiority of waveform diversity, MIMO radar offers great potential in target detection, interference suppression and transmit beampattern synthesis [2]–[5].

It is known that the traditional MIMO radar usually emit perfectly orthogonal waveforms through the transmit antennas. The radiated energy is thus uniformly distributed in whole spatial domain. This will certainly limit the signal-to-interference-plus-noise ratio (SINR) at the receive terminal. To overcome this limitation, the cross-correlation of transmit waveform sequences can be utilized to achieve desired transmit beampattern. Generally speaking, existing pattern design schemes can be classified as the following two categories.

This work was supported in part by the Guangdong Basic and Applied Basic Research Foundation under grants 2020A1515010410 and 2018A030310576, in part by the National Natural Science Foundation of China under grants 61771316 and 61901273, in part by the Guangdong Special Support Program, in part by the Department of Education of Guangdong Province under Grant 2018KTSX195, and in part by the Foundation of Shenzhen under Grant JCYJ20190808114213987.

The first kind of approaches are known as match design, which aim to adapt the cross-correlation information of transmit waveform to minimize the difference between the true and desired beampatterns [6]–[11]. The problem was first considered in terms of synthesizing the signal cross-correlation to approximate the prescribed beampattern [6], which results in a constrained optimization problem that can be solved by interior-point methods. However, recovering signal sequences from the correlation matrix is still a challenging issue. To this end, the one-step cyclic algorithm (CA) was established in [7]. On this basis, a modified match scheme is reported in [11] for constant modulus (CM) waveform design.

The second category focuses on designing the transmit waveform to maximize the radiated energy within the mainlobe region and minimize it elsewhere [12]–[15]. In particular, the preferable performance can be attained by minimizing the integrated sidelobe to mainlobe ratio (ISMR) [12]. To further improve the robustness, the worst case peak sidelobe level (PSL) optimization method [13] is considered to tackle steering vector mismatch. Recently, the spectral coexist of MIMO radar and communication is introduced in [15]. By simultaneously optimizing the ISMR and energy over space-frequency bands, the resulting waveform shows great ability of cooperation between MIMO radar and communication system.

Note that aforementioned beampattern design algorithms were developed for MIMO radar with high-resolution digital-to-analog converters (DACs). In some modern systems, especially large-scale MIMO systems, low-resolution components such as one-bit DACs are deployed. In this case, the above approaches cannot be directly applied. To that end, in this paper, we consider synthesizing the transmit waveform, which consists of binary symbol quantized by one-bit DACs, to minimize the ISMR. By doing so, the transmitted energy can be focused into the mainlobe region, with minimized leakage power in the sidelobe is also minimize. The effectiveness of this method is validated by simulation results.

II. PROBLEM FORMULATION

Consider a monostatic MIMO radar system equipped with M transmit antennas, distributed as a uniform linear array with half-wavelength inter-element spacing. At the l -th time instant, the vector of transmit signal can be expressed as

$\mathbf{s}_l = [s_1(l), s_2(l), \dots, s_M(l)]^T \in \mathbb{C}^M$, where $s_m(l)$ denotes the signal transmitted by the m -th element. In order to reduce the complexity of RF chains, we assume that a pair of one-bit DACs are deployed for each channel to quantize the real and imaginary components of the complex signal, respectively. Hence, the resulting 1-bit waveform sequence, which stacked by a vector form, can be denoted as

$$\mathbf{x} = [\mathbf{x}_1^T, \mathbf{x}_2^T, \dots, \mathbf{x}_L^T]^T \in \mathbb{C}^{ML}, \quad \mathbf{x}_l = \mathcal{Q}_C(\mathbf{s}_l) \quad (1)$$

where L is the number of discrete time samples and $\mathcal{Q}_C(\cdot) = \mathcal{Q}(\cdot) + j\mathcal{Q}(\cdot)$ denotes the complex-valued one-bit quantizer. The total power of transmitter, denoted by E , can be expressed as

$$\|\mathbf{x}\|^2 = \sum_{l=1}^L \|\mathbf{x}_l\|^2 = E \quad (2)$$

and thus \mathbf{x} belongs to the QPSK constellation given by

$$\mathcal{X} = \left\{ \pm \sqrt{\frac{E}{2ML}} \pm j \sqrt{\frac{E}{2ML}} \right\}. \quad (3)$$

Based on the above model, the synthesized signal at the angle of θ corresponding to the L samples can be written as

$$\begin{aligned} \mathbf{y}(\theta) &= [\mathbf{a}^T(\theta)\mathbf{x}_1, \mathbf{a}^T(\theta)\mathbf{x}_2, \dots, \mathbf{a}^T(\theta)\mathbf{x}_L]^T \\ &= (\mathbf{I}_L \otimes \mathbf{a}^T(\theta))\mathbf{x} \end{aligned} \quad (4)$$

where $\mathbf{a}(\theta) = [1, e^{-j\pi \sin(\theta)}, \dots, e^{-j\pi(M-1)\sin(\theta)}]^T$ denotes the steering vector of the transmit antenna array. Accordingly, the transmit beampattern can be characterized by the spatial power spectrum as

$$P(\theta) = \mathbf{y}^H(\theta)\mathbf{y}(\theta) = \mathbf{x}^H(\mathbf{I}_L \otimes \mathbf{a}^*(\theta)\mathbf{a}^T(\theta))\mathbf{x}. \quad (5)$$

Described as previous section, the transmit energy is expected to be concentrated into the mainlobe region Θ_m as much as possible [8]–[15]. Noted that Θ_m may be composed of sub-regions, i.e., multiple beams. According to (5), the quality of energy focusing is quantified in terms of the integrated sidelobe to mainlobe ratio (ISMR) defined as

$$\text{ISMR} = \frac{\int_{\Theta_s} \mathbf{x}^H(\mathbf{I}_L \otimes \mathbf{a}^*(\theta)\mathbf{a}^T(\theta))\mathbf{x}d\theta}{\int_{\Theta_m} \mathbf{x}^H(\mathbf{I}_L \otimes \mathbf{a}^*(\theta)\mathbf{a}^T(\theta))\mathbf{x}d\theta} = \frac{\mathbf{x}^H \boldsymbol{\Omega}_s \mathbf{x}}{\mathbf{x}^H \boldsymbol{\Omega}_m \mathbf{x}} \quad (6)$$

where Θ_s denotes the sidelobe region, $\boldsymbol{\Omega}_s$ and $\boldsymbol{\Omega}_m$ are defined, respectively, as

$$\boldsymbol{\Omega}_s = \mathbf{I}_L \otimes \mathbf{A}(\Theta_s), \quad \boldsymbol{\Omega}_m = \mathbf{I}_L \otimes \mathbf{A}(\Theta_m) \quad (7)$$

and the integral $\mathbf{A}(\Theta) \triangleq \int_{\Theta} \mathbf{a}^*(\theta)\mathbf{a}^T(\theta)d\theta$ over Θ (either Θ_m or Θ_s) can be numerically computed.

Recalling the above requirements, the following optimization problem can be formulated

$$\min_{\mathbf{x}} \frac{\mathbf{x}^H \boldsymbol{\Omega}_s \mathbf{x}}{\mathbf{x}^H \boldsymbol{\Omega}_m \mathbf{x}}, \quad s.t. \quad \mathbf{x} \in \mathcal{X} \quad (8)$$

which is, however, difficult to tackle because of the quadratic fractional function and discrete constraint. Towards that end, an ADMM-based solver will be introduced in the sequel.

III. THE ADMM-BASED SOLVER

To facilitate dealing with the problem (8), we first transform it into real-valued form expressed as

$$\min_{\mathbf{x}_r} \frac{\mathbf{x}_r^T \boldsymbol{\Omega}_{s,r} \mathbf{x}_r}{\mathbf{x}_r^T \boldsymbol{\Omega}_{m,r} \mathbf{x}_r}, \quad s.t. \quad \mathbf{x}_r \in \mathcal{X}_r \quad (9)$$

where $\mathbf{x}_r = [\Re\{\mathbf{x}\}^T, \Im\{\mathbf{x}\}^T]^T$, $\mathcal{X}_r = \{\pm\sqrt{E/2ML}\}$,

$$\boldsymbol{\Omega}_{s,r} = \begin{bmatrix} \Re\{\boldsymbol{\Omega}_s\} & -\Im\{\boldsymbol{\Omega}_s\} \\ \Im\{\boldsymbol{\Omega}_s\} & \Re\{\boldsymbol{\Omega}_s\} \end{bmatrix} \quad (10)$$

and $\boldsymbol{\Omega}_{m,r}$ is similarly defined.

To begin with, let us present an essential variable reformulation [16].

Lemma 1: Let $\Upsilon \triangleq \{(\mathbf{e}, \mathbf{x}_r) \mid \mathbf{e} - \mathbf{x}_r = \mathbf{0}, \|\mathbf{x}_r\|_\infty \leq \sqrt{\frac{E}{2ML}}, \|\mathbf{e}\|^2 = E\}$ and assume that $(\mathbf{e}, \mathbf{x}_r) \in \Upsilon$, then we have $\mathbf{e} \in \mathcal{X}_r$ and $\mathbf{x}_r \in \mathcal{X}_r$.

Based on Lemma 1, the problem (9) can be rewritten as

$$\min_{\mathbf{e}, \mathbf{x}_r} \frac{\mathbf{e}^T \boldsymbol{\Omega}_{s,r} \mathbf{e}}{\mathbf{e}^T \boldsymbol{\Omega}_{m,r} \mathbf{e}} \quad (11a)$$

$$s.t. \quad \mathbf{e} - \mathbf{x}_r = \mathbf{0} \quad (11b)$$

$$\|\mathbf{e}\|^2 = E \quad (11c)$$

$$\mathbf{x}_r \in \mathcal{D} \quad (11d)$$

where $\mathcal{D} \triangleq \left[-\sqrt{\frac{E}{2ML}}, \sqrt{\frac{E}{2ML}}\right]$ indicates that we relax the discrete binary constraint to continuous interval. Thus, the augmented Lagrangian function of problem (11) is given by

$$\mathcal{L}(\mathbf{e}, \mathbf{x}_r, \mathbf{w}, \rho) = F(\mathbf{e}) + \mathbf{w}^T(\mathbf{e} - \mathbf{x}_r) + \frac{\rho}{2}\|\mathbf{e} - \mathbf{x}_r\|^2 \quad (12)$$

where \mathbf{w} is the Lagrangian multipliers, $\rho > 0$ denotes the penalty parameter and $F(\mathbf{e})$ is given by

$$F(\mathbf{e}) = \frac{\mathbf{e}^T \boldsymbol{\Omega}_{s,r} \mathbf{e}}{\mathbf{e}^T \boldsymbol{\Omega}_{m,r} \mathbf{e}}. \quad (13)$$

Under ADMM framework, we consider to minimize the $\mathcal{L}(\mathbf{e}, \mathbf{x}_r, \mathbf{w}, \rho)$ with respect to the fixed value of variables. In each iteration, the alternating gradient descent method is used to update the estimation of \mathbf{e} , \mathbf{x}_r and \mathbf{w} . Specifically, the update procedure of ADMM can be given by

$$\mathbf{e}^{(t+1)} = \underset{\mathbf{e}}{\text{argmin}} \mathcal{L}(\mathbf{e}, \mathbf{x}_r^{(t)}, \mathbf{w}^{(t)}, \rho) \quad (14a)$$

$$\mathbf{x}_r^{(t+1)} = \underset{\mathbf{x}_r \in \mathcal{D}}{\text{argmin}} \mathcal{L}(\mathbf{e}^{(t+1)}, \mathbf{x}_r, \mathbf{w}^{(t)}, \rho) \quad (14b)$$

$$\mathbf{w}^{(t+1)} = \mathbf{w}^{(t)} + \rho(\mathbf{e}^{(t+1)} - \mathbf{x}_r^{(t+1)}) \quad (14c)$$

Next, we will introduce the solution of subproblem (14a) and (14b) in detail.

Update of \mathbf{e} : We first consider to update the \mathbf{e} with the fixed value of $\{\mathbf{x}_r^{(t)}, \mathbf{w}^{(t)}\}$. The problem (14a) can be formulated as

$$\min_{\mathbf{e}} F(\mathbf{e}) + \mathbf{w}^{(t)T}(\mathbf{e} - \mathbf{x}_r^{(t)}) + \frac{\rho}{2}\|\mathbf{e} - \mathbf{x}_r^{(t)}\|^2 \quad (15)$$

$$s.t. \quad \|\mathbf{e}\|^2 = E.$$

Due to the quadratic fractional function $F(\mathbf{e})$, this problem cannot be analytically solve. Fortunately, as shown in [15], the

problem of (15) can be efficiently tackled in an approximation manner. More precisely, given the current point $\mathbf{e}^{(t)}$, the first-order Taylor series approximation of $F(\mathbf{e})$ is

$$F^\dagger(\mathbf{e}) = F(\mathbf{e}^{(t)}) + \nabla^T F(\mathbf{e}^{(t)})(\mathbf{e} - \mathbf{e}^{(t)}) \quad (16)$$

where

$$\nabla F(\mathbf{e}) = \frac{2(\boldsymbol{\Omega}_{s,r}\mathbf{e} - F(\mathbf{e})\boldsymbol{\Omega}_{m,r}\mathbf{e})}{\mathbf{e}^T \boldsymbol{\Omega}_{m,r}\mathbf{e}}. \quad (17)$$

Replacing $F(\mathbf{e})$ by $F^\dagger(\mathbf{e})$, the optimization problem (15) can be rewritten as

$$\begin{aligned} \min_{\mathbf{e}} \quad & F^\dagger(\mathbf{e}) + \mathbf{w}^{(t)T}(\mathbf{e} - \mathbf{x}_r^{(t)}) + \frac{\rho}{2}\|\mathbf{e} - \mathbf{x}_r^{(t)}\|^2 \\ \text{s.t.} \quad & \|\mathbf{e}\|^2 = E. \end{aligned} \quad (18)$$

By setting the derivative of objective function of problem (18) to zero with respect to \mathbf{e} , we obtain

$$\nabla F(\mathbf{e}^{(t)}) + \mathbf{w}^{(t)} + \rho(\mathbf{e} - \mathbf{x}_r^{(t)}) = \mathbf{0}. \quad (19)$$

After some manipulations and recalling the power constraint of (18), we can then update \mathbf{e} as follows

$$\mathbf{e}^{(t+1)} = \sqrt{E} \frac{\tilde{\mathbf{e}}^{(t+1)}}{\|\tilde{\mathbf{e}}^{(t+1)}\|} \quad (20)$$

where $\tilde{\mathbf{e}}^{(t+1)}$ is defined as

$$\tilde{\mathbf{e}}^{(t+1)} = \frac{1}{\rho}(\rho\mathbf{x}_r^{(t)} - \mathbf{w}^{(t)} - \nabla F(\mathbf{e}^{(t)})). \quad (21)$$

Update of \mathbf{x}_r : If we fix the value of $\{\mathbf{e}^{(t+1)}, \mathbf{w}^{(t)}\}$, the optimization problem (14b) is modified as following

$$\begin{aligned} \min_{\mathbf{x}_r} \quad & \mathbf{w}^{(t)T}(\mathbf{e}^{(t+1)} - \mathbf{x}_r) + \frac{\rho}{2}\|\mathbf{e}^{(t+1)} - \mathbf{x}_r\|^2 \\ \text{s.t.} \quad & \mathbf{x}_r \in \mathcal{D}. \end{aligned} \quad (22)$$

It is seen that problem (22) is convex and easy to obtain the closed-form solution in polynomial time. Several efficient methods have been proposed to deal with this kind of problems. Herein, according to the constraint in (22), the proximal gradient algorithm is applied. Similarly, setting the derivative of objective function of problem (22) to zero with respect to \mathbf{x}_r , we obtain

$$\mathbf{w}^{(t)} + \rho(\mathbf{e}^{(t+1)} - \mathbf{x}_r) = \mathbf{0}. \quad (23)$$

Thus, the variable \mathbf{x}_r can be update as

$$\mathbf{x}_r^{(t+1)} = \Pi_{\mathcal{D}} \left(\mathbf{e}^{(t+1)} + \frac{1}{\rho} \mathbf{w}^{(t)} \right) \quad (24)$$

where $\Pi_{\mathcal{D}}(\cdot)$ denotes the projection operator onto set \mathcal{D} .

IV. SIMULATION RESULTS

Throughout our simulations, the transmit array is assumed to be uniform linear array with half-wavelength inter-element spacing. Without loss the generality, the total transmit power is fixed as $E = 1$. The whole spatial direction (i.e., $\theta \in [-90^\circ, 90^\circ]$) is assumed to be uniformly sampled with 1° step-size. The penalty parameters are assumed as $\rho = 10$ and $\sigma = 1.2$. The initial variable $\mathbf{e}^{(0)}$ is selected to be zero-mean and $E/2ML$ variance Gaussian random vector. We set

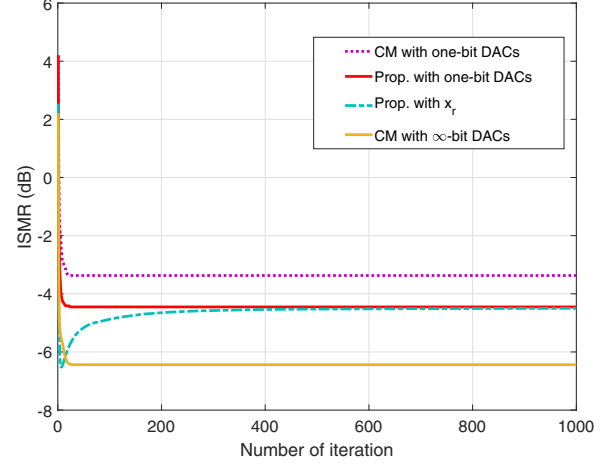


Fig. 1. The value of objective function in (9) versus the number of iteration.

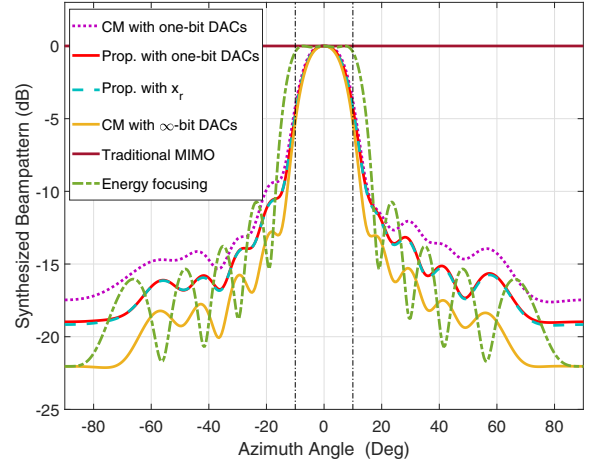


Fig. 2. Comparison of synthesized transmit beampatterns. $M = 12, L = 80$.

$\rho^{(0)} = 10$ and $\sigma = 1.2$. As for the variable $\mathbf{x}_r^{(0)}$ and $\mathbf{v}^{(0)}$, both of them are chosen as zero vector. Finally, the total number of iteration is chosen with $t_{max} = 1000$.

Example 1 : Let us consider $M = 12$ and $L = 80$. And one mainlobe ranged from $[-10^\circ, 10^\circ]$. Fig. 1 expresses the value of objective function in (9) versus the number of iteration. It is seen that the best performance is certainly achieved by constant modulus (CM) waveform design method with ∞ -bit DACs [15]. This is mainly because ∞ -bit DACs have more degrees of freedom for waveform design. Meanwhile, the proposed method with one-bit DACs have at least 1dB performance enhancement compared with CM 1-bit method (quantized the CM ∞ -bit waveform directly). We can also find that the value gap between proposed method and its one-bit quantization is close to zero as the increase of iteration number. This implies that our method can design the perfect one-bit waveform with best ISMR performance. This coincides with the Lemma 1 and validates our analysis.

Fig. 2 compares the synthesized transmit beampatterns of six methods. The number of beam for energy focusing method

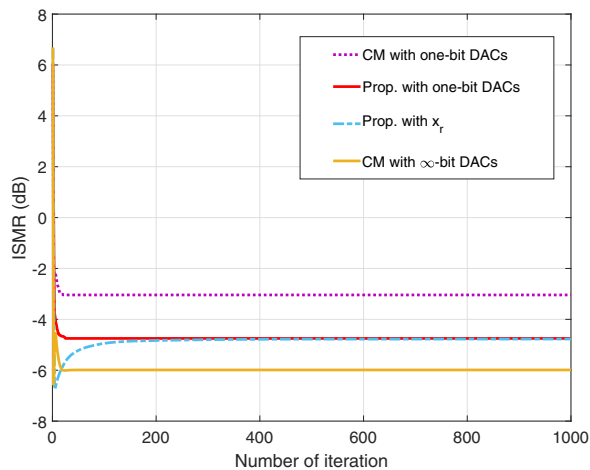


Fig. 3. The value of objective function in (9) versus the number of iteration.

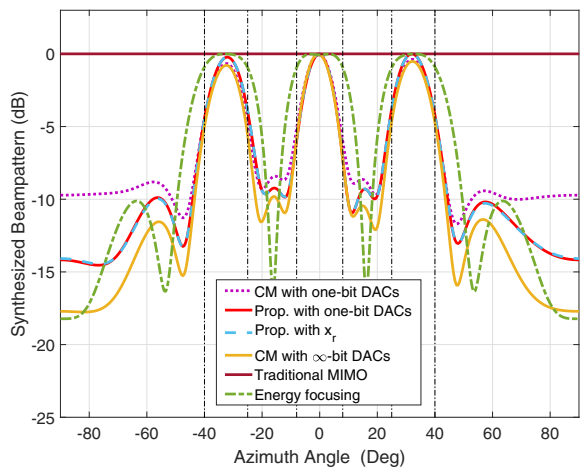


Fig. 4. Comparison of synthesized transmit beampatterns. $M = 10$, $L = 100$.

[4] is chosen as $K = 3$. As shown in Fig. 2, the CM ∞ -bit method achieves the best sidelobe performance due to the flexibility of transmit waveform. Meanwhile, the proposed method can achieve lower sidelobe level compared with CM one-bit method. Lastly, the energy focusing method expresses uniform mainlobe power distribution. However, the leakage power in sidelobe region is also more than others.

Example 2 : We assume $M = 10$ and $L = 100$, and three mainlobes, which ranged from $[-40^\circ, -25^\circ] \cup [-8^\circ, 8^\circ] \cup [25^\circ, 40^\circ]$, are considered. Fig. 3 shows the value of objective function in (9) versus the number of iteration. Similarly, the CM ∞ -bit waveform design method still has the minimum ISMR which means the most of transmit energy was focused into the mainlobe in this case. At the same time, it is also seen that the proposed method achieves 1.7 dB performance enhancement compared with CM 1-bit waveform method which is coincident with Fig. 1. As expectation, the value gap between proposed method and its one-bit quantization is vanish as the increase of iteration number.

Fig. 4 depicts the resulting transmit beampattern for six methods. The number of beam for energy focusing method is chosen as $K = 5$. Once again, the beampattern with CM ∞ -bit waveform acquires the best performance than others. However, under one-bit DACs scenario, the proposed method still has performance gain, such as lower sidelobe can obtain.

V. CONCLUSION

A new transmit beampattern synthesis algorithm for MIMO radar equipped with one-bit DACs is devised. By properly designing the one-bit transmit waveform sequence vector, the synthesized beampattern can minimize the integrated sidelobe to mainlobe ratio (ISMR) to achieve energy focusing. An ADMM-based solver is devised to solve the resulting optimization problem. The effectiveness and improved performance of proposed method are verified by simulation results.

REFERENCES

- [1] R. Kshetrimayum, *Fundamental of MIMO wireless communication*. Cambridge, U.K.: Cambridge Univ. Press, 2017.
- [2] J. Li and P. Stoica, "MIMO radar with colocated antennas," *IEEE Signal Processing Magazine*, vol. 24, no. 5, pp. 106–114, Sept 2007.
- [3] J. Li, P. Stoica, L. Xu, and W. Roberts, "On parameter identifiability of MIMO radar," *IEEE Signal Processing Letters*, vol. 14, no. 12, pp. 968–971, Dec 2007.
- [4] A. Hassanien and S. A. Vorobyov, "Transmit energy focusing for DOA estimation in MIMO radar with colocated antennas," *IEEE Transactions on Signal Processing*, vol. 59, no. 6, pp. 2669–2682, June 2011.
- [5] P. Stoica, J. Li, and Y. Xie, "On probing signal design for MIMO radar," *IEEE Transactions on Signal Processing*, vol. 55, no. 8, pp. 4151–4161, Aug 2007.
- [6] D. R. Fuhrmann and G. S. Antonio, "Transmit beamforming for MIMO radar systems using signal cross-correlation," *IEEE Transactions on Aerospace and Electronic Systems*, vol. 44, no. 1, pp. 171–186, Jan. 2008.
- [7] P. Stoica, J. Li, and X. Zhu, "Waveform synthesis for diversity-based transmit beampattern design," *IEEE Transactions on Signal Processing*, vol. 56, no. 6, pp. 2593–2598, June 2008.
- [8] S. Ahmed, J. S. Thompson, Y. R. Petillot, and B. Mulgrew, "Unconstrained synthesis of covariance matrix for MIMO radar transmit beampattern," *IEEE Transactions on Signal Processing*, vol. 59, no. 8, pp. 3837–3849, Aug 2011.
- [9] G. Hua and S. S. Abeysekera, "MIMO radar transmit beampattern design with ripple and transition band control," *IEEE Transactions on Signal Processing*, vol. 61, no. 11, pp. 2963–2974, June 2013.
- [10] X. Zhang, Z. He, L. Rayman-Bacchus, and J. Yan, "MIMO radar transmit beampattern matching design," *IEEE Transactions on Signal Processing*, vol. 63, no. 8, pp. 2049–2056, April 2015.
- [11] Z. Cheng, Z. He, S. Zhang, and J. Li, "Constant modulus waveform design for MIMO radar transmit beampattern," *IEEE Transactions on Signal Processing*, vol. 65, no. 18, pp. 4912–4923, Sep. 2017.
- [12] H. Xu, R. S. Blum, J. Wang, and J. Yuan, "Colocated MIMO radar waveform design for transmit beampattern formation," *IEEE Transactions on Aerospace and Electronic Systems*, vol. 51, no. 2, pp. 1558–1568, April 2015.
- [13] A. Aubry, A. D. Maio, and Y. Huang, "MIMO radar beampattern design via PSL/ISL optimization," *IEEE Transactions on Signal Processing*, vol. 64, no. 15, pp. 3955–3967, Aug 2016.
- [14] W. Fan, J. Liang, and J. Li, "Constant modulus MIMO radar waveform design with minimum peak sidelobe transmit beampattern," *IEEE Transactions on Signal Processing*, vol. 66, no. 16, pp. 4207–4222, Aug 2018.
- [15] Z. Cheng, C. Han, B. Liao, Z. He, and J. Li, "Communication-aware waveform design for MIMO radar with good transmit beampattern," *IEEE Transactions on Signal Processing*, vol. 66, no. 21, pp. 5549–5562, Nov 2018.
- [16] G. Yuan and B. Ghanem, "Binary optimization via mathematical programming with equilibrium constraints," *arXiv preprint:1608.04425*, Sep 2016.